DOI: 10.1002/hlca.201900046

FULL PAPER

HELVETICA chimica acta

Small Cage Uranofullerenes: 27 Years after Their First Observation

Alejandra Gómez-Torres,[a] Ronda Esper,[a] Paul W. Dunk,*[b] Roser Morales-Martínez,[c] Antonio Rodríguez-Fortea,[c] Luis Echegoyen,*[a] and Josep M. Poblet*[c]

[a] Department of Chemistry University of Texas at El Paso, 500 West University Avenue, El Paso, TX 79968, USA, e-mail: echegoyen@utep.edu

[b] Florida State University, National High Magnetic Field Laboratory, 1800 East Paul Dirac Drive, Tallahassee, FL 32310, USA, e-mail: dunk@magnet.fsu.edu

[c] Departament de Química Física i Inorgànica, Universitat Rovira i Virgili, C/Marcel·lí Domingo 1, ES-43007 Tarragona, Catalonia, Spain, e-mail: josepmaria.poblet@urv.cat

Dedicated to *François Diederich* on the occasion of his retirement

The tetravalently stabilized fullerene cage of C_{28} is historically the most elusive small fullerene cage observed by employing the laser vaporization synthesis methodology. Its first observation reported by *Smalley et al.* in 1992 suggests that C_{28} is potentially the smallest and most stable fullerene ever observed. By using the *Krätschmer–Huffman* arc discharge synthesis method, we have recently succeeded in synthesizing a series of uranium-endohedral fullerenes which differ from those reported by *Smalley* and co-workers. Intrigued by this interesting mismatch, we tuned our experimental conditions to favor the formation and detection of these missing species. Experiments done using solvents of varying polarity allowed the observation of several empty and uranofullerenes. Extractions with pyridine and *o*-DCB allowed for observation of small $U@C_{2n}$ ($2n = 28$, 60, 66, 68, 70) by high resolution *Fourier*-Transform Ion Cyclotron Resonance Mass Spectrometry (FT-ICR MS). This is the first time that $U@C_{28}$ is observed in soot produced by the *Krätschmer-Huffman* arc-discharge methodology. Carbon cage selection and spin density distribution on the endohedral metallofullerenes (EMFs) $U@C_{60}$, $U@C_{70}$, and $U@C_{72}$ were studied by means of density functional theory (DFT) calculations. A plausible pathway for the formation of $U@D_{3h}$-C_{74} from $U@D_{5h}$-C_{70} through two C_2 insertions and one *Stone-Wales* rearrangement is proposed.

Keywords: uranofullerenes, small cage fullerenes, laser ablation, *Krätschmer-Huffman* arc-discharge, solubility, fullerenes.

Introduction

The early seminal work by *Smalley et al.* on the observation of uranium endofullerenes spurred investigations about these nanoscale uranium containing carbon structures to better understand their electronic and chemical properties.[1] Despite much investigation, the isolation of uranium endohedral metallofullerenes (EMFs) remained an elusive goal for scientists for several years. Very recently, we reported a couple of experimental investigations that led to the isolation and structural characterization by X-Ray crystallography of the first examples of mono-uranium EMFs, the IPR cages $U^{4+}@D_{3h}$-C_{74}^{4-}, $U^{4+}@C_2(5)$-C_{82}^{4-}, and $U^{3+}@C_{2v}(9)$-C_{82}^{3-},[2] as well as the non-IPR cages $U@C_1(17418)$-C_{76} and $U@C_1(28324)$-C_{80}.[3] The mass spectrum in *Figure 1,a* shows the fullerene products reported by *Smalley* and co-workers 27 years ago, while our results are shown in *Figure 1,b*. Note that in *Figure 1,a* small sized mono-uranofullerenes $U@C_{28\text{-}72}$ are predominant, while spectrum *1,b* only exhibits mono-uranofullerenes bigger than $U@C_{72}$. The specificity of our experimental set up, which incorporates reactive gases such as H_2 and NH_3, leads to the additional formation of dimetallic and cluster endohedral compounds.

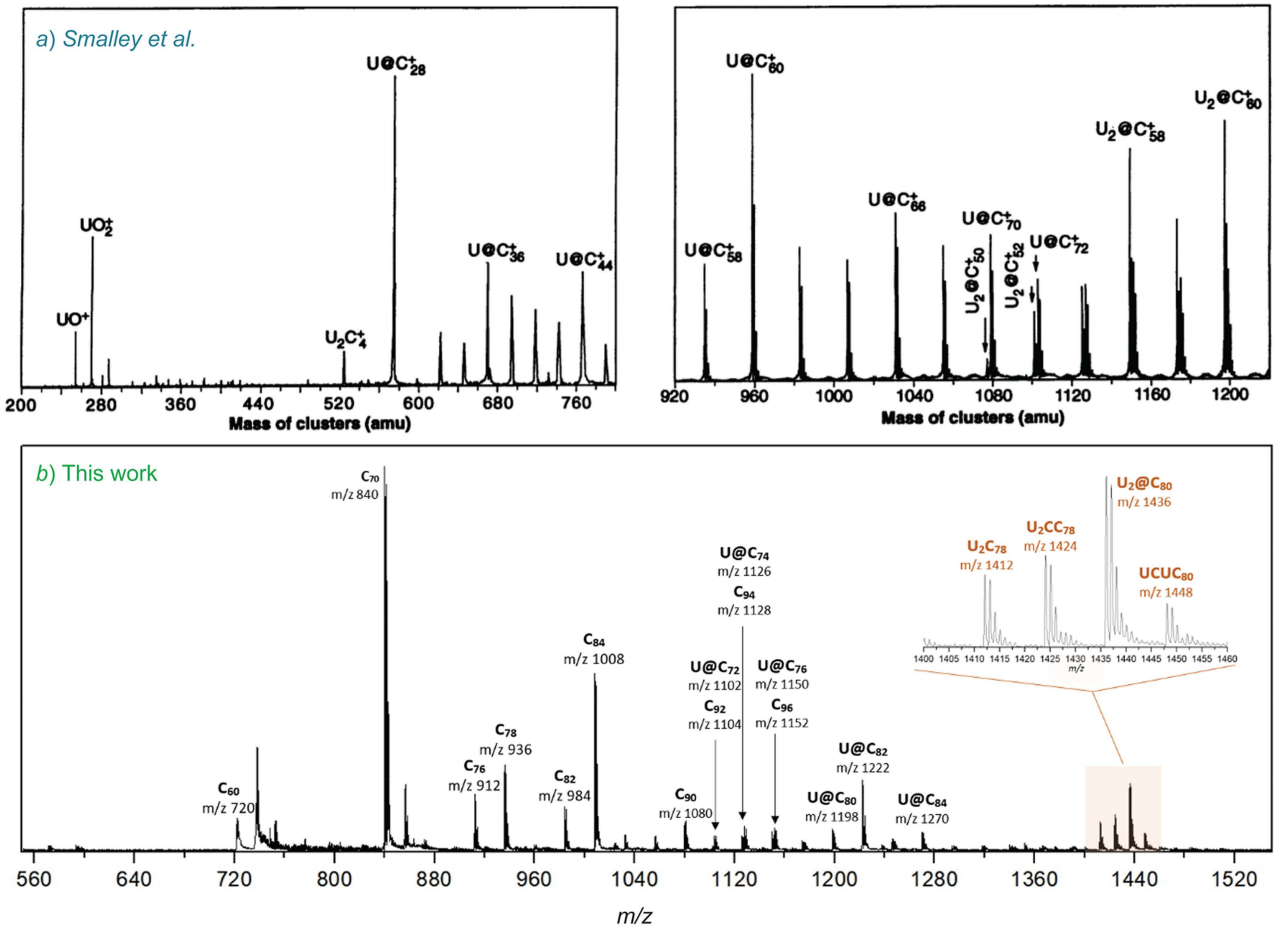

Figure 1. Fullerene synthesis products observed by *a*) *Smalley et al.* using FT-ICR mass spectrometry and *b*) us using LDI-TOF positive-ion mass spectrometry.

The discrepancies observed in *Figure 1*, clearly indicate that there are multiple factors guiding the formation of small mono-metallic endohedrals. For instance, there is a correlation between the synthesis methodology used and the growth mechanism of the fullerene cages formed.[4] In a recent study reported by *Dunk et al.*, laser ablation, the same synthetic method used by *Smalley* and co-workers, was used in the synthesis of M@C_{28} (M=Ti, Zr, and U) species.[5] Their work provided further insight into the formation mechanism of uranofullerenes, demonstrating the role of the smallest stable species U@C_{28} as the precursor for larger uranofullerenes formed by the bottom-up formation mechanism proposed by *Curl*[6] and further developed by *Dunk et al.*[5,7] Several other investigations have been conducted using the *Krätschmer-Huffman* arc-discharge synthetic method instead.[8] The first case of uranium EMFs synthesized under anaerobic conditions emerged from the early arc-discharge experiments by *Diener* and colleagues.[9] In agreement with *Smalley*'s observations, they were able to detect U@C_{60} by mass spectrometry, but U@C_{28} was not detected even when the soot was analyzed prior to sublimation. It was proposed that the discrepancies observed between both outcomes is a consequence of differences in the condensation of carbon-uranium vapor as a function of the synthetic method employed.[9]

Challenges in the solubilization of small mono-metallic endohedral fullerenes have restricted their observation. These species are believed to be highly reactive open shell systems that become insoluble in the common organic and aromatic solvents typically used for fullerene extraction.[10] It has been demonstrated that many products remain in the soot after extraction of the soluble ones.[11] This behavior was clearly illustrated in the synthesis of La@C_{60}, La@C_{74}, and La@C_{82}, which were clearly detected in the sublimed soot by mass spectrometry, however, when an extraction with toluene was carried out, only

La@C_{82} was successfully observed.[12] Researchers have done extensive work to find the appropriate solvents and methodologies to extract small cage mono-metallofullerenes M@$C_{60\text{-}70}$ from raw carbon soot.[13–16] Examples found in the literature include an exhaustive study involving 48 different solvents, in which M@C_{60} (M=Y, Ba, La, Ce, Pr, Nd, Gd) were successfully extracted with aniline and pyridine.[17] In a separate study, the purification of Er@C_{60} and Eu@C_{60} was successfully achieved upon sublimation followed by sonication in aniline and multistep HPLC.[18,19] *Akasaka et al.* managed to successfully obtain pure Dy@C_{60} from an aniline extract.[20]

Notwithstanding the examples mentioned above, the formation and stability of small-cage mono-metallofullerenes remains poorly understood. Further efforts to probe the origin of their instability have led us to believe these are very reactive species possessing small HOMO-LUMO gap values.[11] EMFs of this nature prefer to oligomerize and thus lead to insoluble species. Several studies have reported that these low HOMO-LUMO gap compounds can be stabilized by electrochemical reduction or radical reagents.[11,13,21–23]

Here we address the discrepancies observed between our and *Smalley*'s results by creating a new experimental set-up suitable for the production and extraction of small cage uranofullerenes. We show that it is possible to produce the stable small species U@C_{2n} ($2n$ = 28, 60, 66, 68, 70) using the arc-discharge technique and to extract them using polar solvents. Computational studies were performed to rationalize these results based on the most stable isomeric cage structures for U@C_{2n} ($2n$ = 60, 70, 72) and spin density distribution calculations.

Results and Discussion

Preparation of EMFs

Synthesis of the raw uranium-carbon soot containing several mono-, di-, and cluster-uranium endohedral fullerenes shown in *Figure 1,b* was carried out using a custom built DC arc discharge generator. Carbon rods (length = 6″, diameter = 3/8″) were initially doped with a U_3O_8 (99.999%)/graphite (99.999%) packing mixture (U/C 1:24 molar ratio). Carbon rods were vaporized under a 200 Torr He, 10 Torr H_2, and 10 Torr NH_3 atmosphere. Positive-ion laser desorption/ionization time-of-flight mass spectrometry measurement (LDI-TOF-MS) was conducted on a *Bruker Microflex LRF* mass spectrometer. Raw soot was extracted under reflux conditions with common solvents used for fullerene extractions like CS_2 and toluene (C_7H_8). As shown in *Figure 1,b*, U@C_{72} is the smallest and U@C_{82} is the most abundant among the mono-uranium endohedrals obtained using this set of conditions. Incorporation of reactive gases induces the formation of di-uranium EMFs U_2C_{78}, U_2C_{79}, $U_2@I_h(7)$-C_{80}[24], and UCU@$I_h(7)$-C_{80}.[25]

Having made these observations, we turned our attention towards the synthesis and extraction of smaller uranofullerenes. To afford the latter, the synthetic experimental procedure and the extraction approach were modified. Bigger carbon rods (length = 7″, diameter = 1/2″) were used to enable higher current values (140–180 Å) and thus higher temperatures in the plasma.[26] To favor the formation of monometallic species over cluster EMFs and hydrocarbons, additional reactive gases such us NH_3 and H_2 were not used. Raw soot extracted using *o*-DCB was analyzed using high resolution *Fourier* transform ion cyclotron resonance (FT-ICR) mass spectrometry in a custom-built FT-ICR mass spectrometer based on a 9.4T superconducting magnet performed with positive ions. For this, a raw soot/o-DCB suspension was applied directly to the surface of a quartz target rod for laser desorption. Molecular ions were generated without a matrix using a Nd:YAG (532 nm, 1–2 mj/pulse) laser. Results are presented in *Figure 2*.

Significantly, small U@C_{2n} ($2n$ = 28, 60, 66, 68, 70) species were successfully synthesized and extracted from the raw soot. Experimental isotopic distributions of all observed EMFs and empty fullerenes display excellent agreement with the calculated ones. It can be inferred from *Figure 2* that the relative abundance of empty carbon cages is higher than for any mono-uranium EMF. Low abundance of U@C_{66} and U@C_{68} is observed. Interestingly, a significant enhancement is observed in the relative abundance of U@C_{28}, U@C_{60}, and U@C_{70}, and the smallest molecule is the most abundant among the new species. Further, the results are consistent with observations made by *Dunk et al.* in a previous study.[5] Encapsulated tetravalent cations, such as Ti or U are capable of transferring enough electrons to the cage with only 28 carbon atoms thus stabilizing its T_d symmetric isomeric cage structure, a configuration that violates the isolated pentagon rule (IPR) by having three fused pentagons.[1,5]

It is interesting to note that whereas in the laser ablation experiments of *Smalley et al.* small cages ($C_{28\text{-}72}$) are formed in high relative abundance, in the arc discharge generation procedure, since the concentration of carbon in the plasma is much higher, the formation of larger cages is favored instead (see *Figure 3*). In addition,

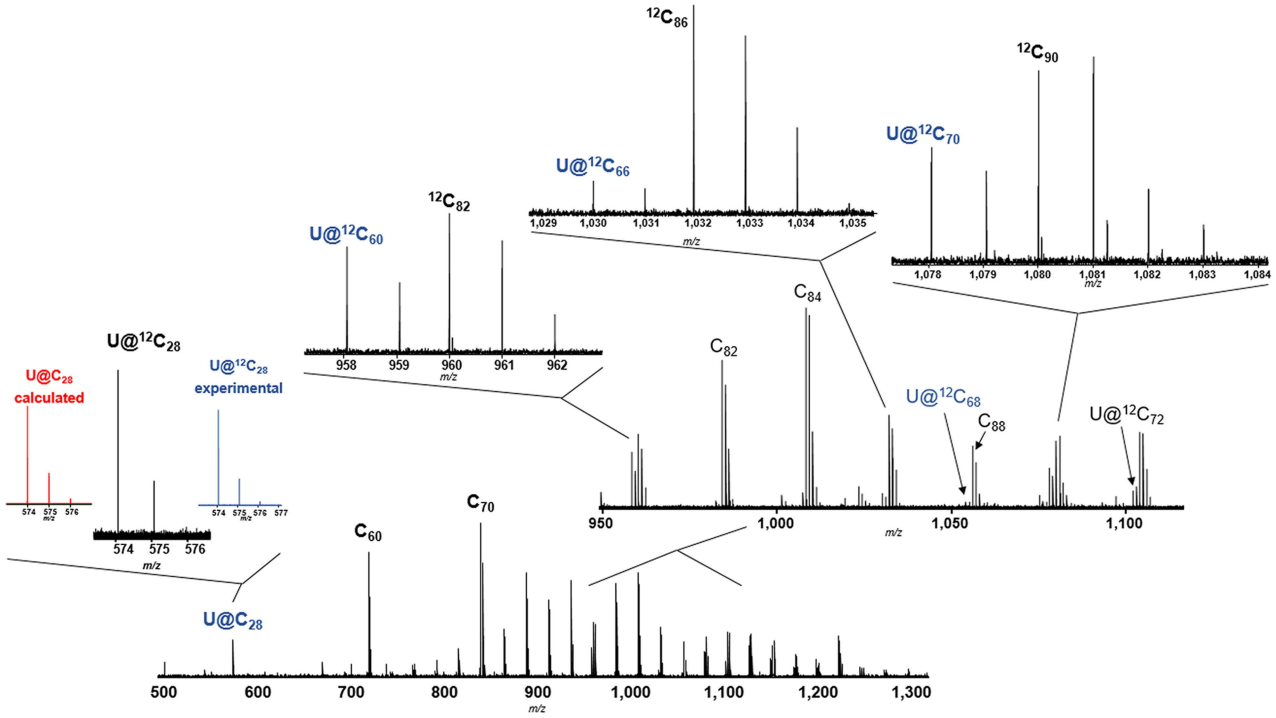

Figure 2. High resolution *Fourier* transform ion cyclotron resonance (FT-ICR) mass spectrum of the crude soot/*o*-DCB suspension positive ions.

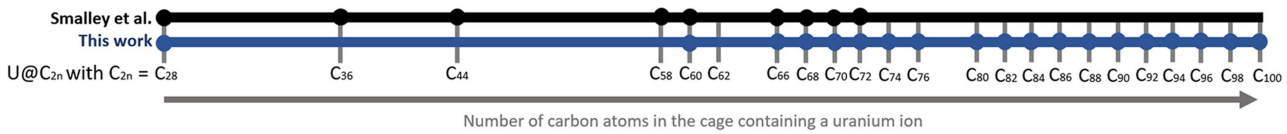

Figure 3. Comparison of the carbon cages containing a single uranium atom observed by *Smalley* and co-workers *vs.* this work.

we note that our result shows a gap between U@C_{28} and U@C_{60}, in which *Smalley* and co-workers observed three EMFs U@C_{2n} ($2n = 36$, 44, 58). Uranofullerenes U@C_{36} and U@C_{44} have been previously described as 'magic numbered' cages possessing enhanced stability compared to other neighboring cages formed by the addition of C_2 or C_3 units through a bottom-up growing mechanism.[7,27]

Solubility Study

It is known that both empty fullerene cages and EMFs show relatively high solubility in a wide variety of organic and aromatic solvents such CS_2 and C_7H_8. In general, EMFs are not as soluble as empty cages. It has been demonstrated that the nature of the solvent affects the extraction efficiency of the more polar metallofullerenes compared to empty fullerenes.[28] To survey the viability of extraction, six solvents commonly used for fullerenes were tested. As such, aniline, pyridine, *o*-DCB, *p*-xylene, C_7H_8, and CS_2 were used for this study (in order of decreasing polarity). LDI-TOF positive-ion mass spectra of the unfiltered uranium-carbon crude suspensions after 15 hours of extraction using the different extraction solvents reveal the presence of relatively intense peaks corresponding to the small uranofullerenes U@C_{2n} ($2n = 60$, 66, 68, 70) in pyridine and *o*-DCB extracts. The smallest mono-uranium species U@C_{28} is almost undetectable by LDI-TOF MS but the ultrahigh resolution offered by FT-ICR MS enabled its unambiguous identification in the pyridine and *o*-DCB extracts with a mass accuracy of parts per billion [ppb]. Going down the polarity scale, the mass spectrum of the *p*-xylene extract displays a significant drop in the relative intensity of the peaks corresponding to U@C_{60} and U@C_{70}, while U@C_{2n} ($2n = 66$, 68) are not observed. U@C_{60} and U@C_{70} signals are considerably lower in intensity for the

extract in toluene, becoming completely undetectable upon extraction with CS_2. We also find the more polar solvent aniline completely ineffective at extracting fullerenes from our soot. These results provide experimental insight into how the encapsulated metal ion enhances the polarity of specific fullerene cages, and consequently their solubility in more polar solvents; as previously reported.[16,17,19,20]

Upon filtration of the uranium-carbon crude suspension, a drastic change was observed by mass spectrometry. The relative intensities of the peaks corresponding to $U@C_{2n}$ ($2n = 28, 60, 66, 68, 70$), which were mainly observed for the *o*-DCB and pyridine extracts, were found to drop dramatically, particularly in the case of $U@C_{28}$ which was not longer observed upon filtration. *Figure 4* shows a representative example, the spectra corresponding to the sample in *o*-DCB prior and after filtration. While $U@C_{60}$ is hardly observed upon filtration, $U@C_{70}$ happens to have a drastic drop in intensity. Interestingly, the availability of the more stable and abundant $U@C_{72}$ species is also affected by its different solubility in *o*-DCB. The $U@C_{72}$ peak shows a smaller but still significant decrease in intensity upon filtration. Small metallofullerenes $M@C_{2n}$ ($2n \leq 70$), like the examples studied in this work, have been largely overlooked because they are usually undetectable when the arc-discharge generation is the chosen method for synthesis.[13,21] The difficulty to extract $M@C_{60}$ and $M@C_{70}$ metallofullerenes has been explained in terms of their instability in air and common solvents.[3,13] In spite of our efforts to successfully produce, detect, and extract these unstable small $U@C_{2n}$ ($2n < 70$) species, further separation using high performance liquid chromatography (HPLC) was not pursued due to the low concentration of the targeted compounds in the sample upon filtration, their low solubility in common HPLC solvents like toluene and the complications of performing HPLC using *o*-DCB as the mobile phase. Further experimental and theoretical studies are necessary to efficiently target their separation and to face the limitations listed.

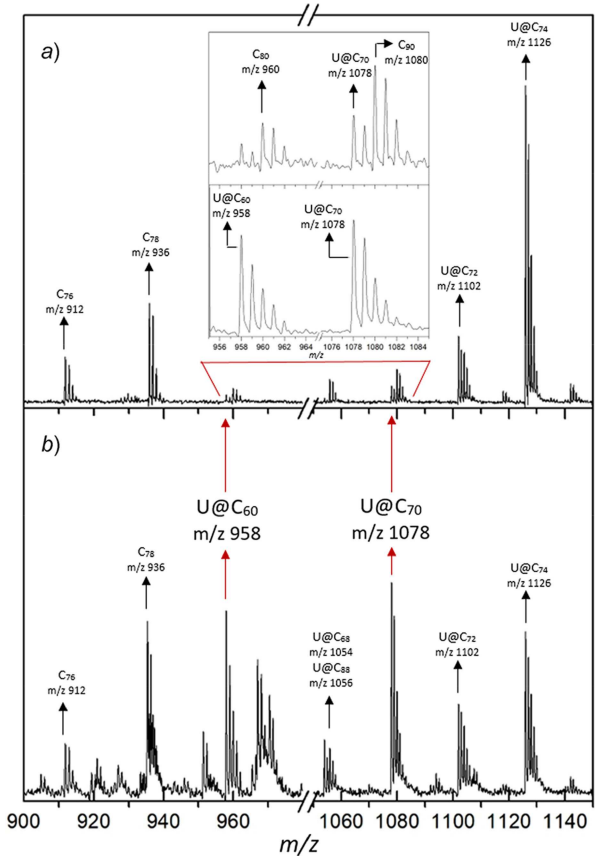

Figure 4. LDI-TOF positive-ion mass spectra corresponding to the arc-discharge synthesis of uranium-containing carbon rods. *a*) Filtered solution of crude soot in *o*-DCB and *b*) unfiltered suspension in *o*-DCB.

DFT Calculations

DFT calculations were carried out for $U@C_{60}$, $U@C_{70}$, and $U@C_{72}$ in order to evaluate what kind of structures is selected by the U atom in these relatively small carbon cages. For $U@C_{60}$, the IPR isomer has the lowest energy, while the unique APP2 isomer has a relative energy of $+13.4\ kcal\,mol^{-1}$. Despite this difference, the predicted molar fractions show that below 1000 K, the IPR isomer is clearly the predominant species, but above this temperature, the 1809 isomer increases in abundance and the molar fractions cross at about 1800 K (*Figure 5*). A similar behavior is observed for $U@C_{70}$, for which the crossing point occurs before 1500 K. In the case of $U@C_{72}$, the situation is different, since the IPR isomer of D_{6h} symmetry is much less stable and there are two non-IPR isomers of C_2 and C_{2v} symmetry, which are significantly lower in energy (see *Table 1*). For a deeper discussion on the origin of the relative stabilization of non-IPR cages at high temperatures see [3].

We have also explored the spin density distributions for these compounds which are compiled in *Figure 6* together with molecular electrostatic potential (MEP) maps and computed dipole moments. *Figure 6* shows how, for some isomers, the spin density is more localized over the carbon cage than for others. Those species with the spin density on the fullerene cage are more reactive and prone to oligomerize. Thus they can be much more difficult to extract from the soot. In

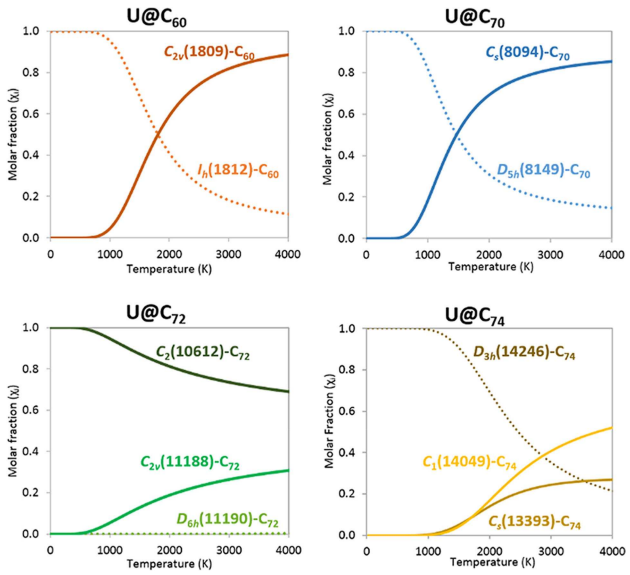

Figure 5. Computed molar fraction as a function of the temperature [K] using the free-encapsulating model (FEM)[29,30] for the lowest-energy isomers for four EMFs U@ C_{2n} with $2n = 60$, 70, 72, and 74. Dashed and continuous lines are used for IPR and non-IPR isomers, respectively.

Table 1. Relative energies computed for selected isomers of U@C_{2n}, $2n = 60$, 70, 72 and 74.

Species	Isomer	Symmetry	APP	ΔE[a]
U@C_{60}	1812	I_h	0	0.0
	1809	C_{2v}	2	13.4
U@C_{70}	8149	D_{5h}	0	0.0
	8094	C_s	1	9.5
U@C_{72}	11190	D_{6h}	0	28.4
	10612	C_2	1	0.0
	11188	C_{2v}	1	6.4
U@C_{74}	14246	D_{3h}	0	0.0[b]
	13393	C_s	1	14.8[b]
	14049	C_1	1	20.1[b]

[a] All the energies correspond to triplet states except for U@C_{72} (11188), in which the quintet state is 0.4 kcal mol^{-1} lower in energy than the triplet. [b] Energy values taken from reference [3].

addition, it has already been mentioned the effect of the solvent polarity in the process of fullerene extraction. As shown in the molecular electrostatic potential representations given in *Figure 6*, the polarity of the fullerene is quite important when an actinide ion is encapsulated inside the fullerene cage, and this polarity is higher for the non-IPR isomers. Computed dipole moments demonstrate that, in general, non-IPR actinide EMFs display larger values.

From the present analysis, we can conclude that in both synthetic techniques, laser ablation and arc discharge vaporization, the peaks observed in the mass spectra for U@C_{72} must correspond to a non-IPR EMF, while for U@C_{60} and U@C_{70}, IPR and non-IPR could be formed. The final isolation from the soot depends also on the possible oligomerization of the fullerene, as well as on the solvent used. It is noteworthy to remark that in the U@C_{2n} series, the U@C_{74} is the smallest most abundant species detected up to now. Indeed, U@D_{3h}-C_{74} is the first IPR cage that is clearly more abundant over a wide temperature range. A possible pathway for the formation of the IPR U@D_{3h}-C_{74} from U@D_{5h}-C_{70} is represented in *Figure 7*, which emphasizes that both IPR isomers are linked by only two C_2 insertions and one *Stone-Wales* (SW) transformation.

Detailed analysis for C_2 insertions in endohedral fullerenes have been reported for several systems.[31,32] The direct link between IPR cages with 70 and 74 carbon atoms suggest that in the case that U@D_{5h}-C_{70} was formed, it could easily grow to give the most stable IPR isomer with 74 carbon atoms. This means that the IPR U@C_{70} isomer will be quite difficult to capture since it will form in low abundance and will tend to grow.

Computational Details

Geometry optimizations were carried out using density functional theory (DFT) with the ADF 2017 package.[33] The PBE functional and *Slater* triple-zeta polarization basis sets were used, including *Grimme* dispersion corrections.[34] Frozen cores consisting of the 1s shell for C and the 1s to 5d shells for U were described by means of single *Slater* functions. Scalar relativistic corrections were included by means of the ZORA formalism. A data set collection of computational results is available in the ioChem-BD repository[35] and can be accessed through https://doi.org/10.19061/iochem-bd-2-35.

Conclusions

Despite a long journey from the first studies on fullerenes, there are still many unknowns about the formation mechanisms of these species. Here, we have discussed some of the different results obtained depending on whether the experiments are conducted out using either laser ablation or arc-discharge

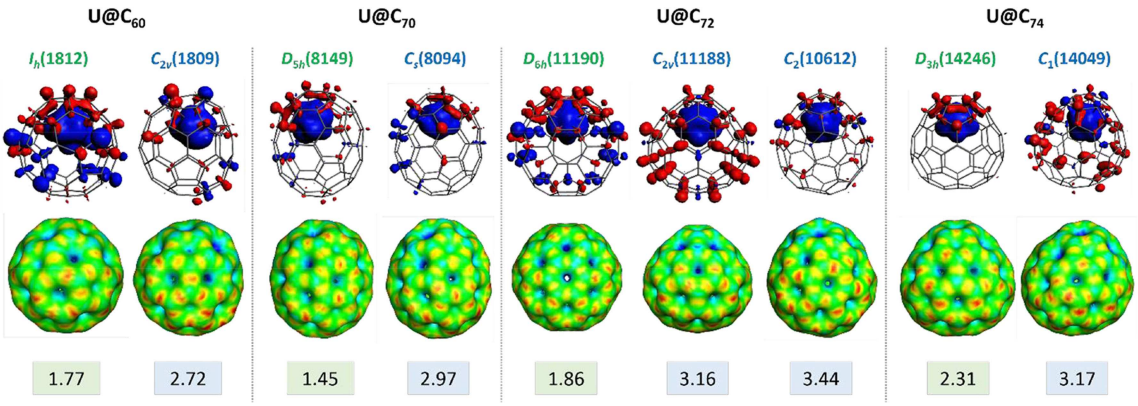

Figure 6. Spin density distributions, molecular electrostatic potential maps and dipole moments (in Debye), for several uranium endohedral fullerenes. Label of the cages are given in green (IPR) and blue (non-IPR).

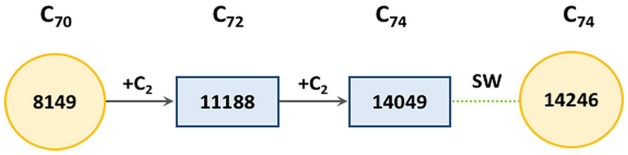

Figure 7. Growth pathway between the two IPR EMFs U@D_{5h}-C_{70} to U@D_{3h}-C_{74}. Circles denote IPR and rectangles denote non-IPR cages.

techniques. We experimentally demonstrate the formation of small uranofullerenes, including the unique U@C_{28} using the arc-discharge method. Extraction of fresh raw soot in six solvents of different polarity revealed a trend for the solvent-extractability of the species here synthesized, small cages stabilized by charge transfer from the internal uranium ion to the cage are more polarized than larger metallofullerenes. Significant changes were observed by means of mass spectrometry measurements upon filtration of the crude, possibly as a result of oligomerization. Non-IPR isomers were found to display higher polarity values over IPR isomers based on dipole moment calculations. Theoretical calculations identify IPR isomers U@I_h(1812)-C_{60} and U@D_{5h}(8149)-C_{70} as the lowest in energy EMFs for U@C_{60} and U@C_{70}, respectively. Nevertheless, at temperature formation of fullerenes the non-IPR isomers U@C_{2v}(1809)-C_{60} and U@C_s(8094)-C_{70} will be very probably more abundant. The most stable conformation for U@C_{72} was predicted to be a non-IPR isomer.

Acknowledgements

We are grateful to *Jesse Murillo* for preliminary research results in the project. Research reported in this article was supported by the *US National Science Foundation* (NSF), we are grateful for their generous support under CHE1801317. The *Robert A. Welch Foundation* is also gratefully acknowledged for an endowed chair to *L. E.* (grant AH-0033). A portion of this work was performed at the National High Magnetic Field Laboratory, which is supported by the NSF Cooperative Agreement through DMR-11-57490 and the State of Florida. *J. M. P.* and *A. R.-F.* thank the Spanish Ministry of Science (grant CTQ2017-87269-P) and the Generalitat de Catalunya (grant 2017SGR629) for support. *J. M. P.* also thanks ICREA foundation for an ICREA ACADEMIA award. *R. M.-M.* thanks Spanish Ministry of Science for a PhD fellowship. Finally, we also thank the National Institute of General Medical Sciences of the National Institutes of Health under linked Award Numbers RL5GM118969, TL4GM118971, and UL1GM118970 for the support received. The content is solely the responsibility of the authors and does not necessarily represent the official views of the National Institutes of Health.

Author Contributions

Alejandra Gómez-Torres performed the synthesis of the raw uranium-carbon soot and wrote the corresponding results and discussion section, in addition to the conclusion. *Ronda Esper* conducted preliminary experiments along with *Jesse Murillo* in addition to writing the abstract and introduction. *Paul W. Dunk* contributed the high resolution *Fourier* transform ion cyclo-

tron resonance (FT-ICR) mass spectral data. *Roser Morlales-Martínez*, *Josep M. Poblet*, and *Antonio Rodríguez-Fortea* conducted DFT calculations and wrote the results and discussion corresponding to their contribution. *Luis Echegoyen* guided the intellectual progress of the article along with providing the laboratory space and materials for the synthesis of the raw uranium-carbon soot.

References

[1] T. Guo, M. D. Diener, Y. Chai, M. J. Alford, R. E. Haufler, S. M. McClure, T. Ohno, J. H. Weaver, G. E. Scuseria, R. E. Smalley, 'Uranium Stabilization of C_{28}: A Tetravalent Fullerene', *Science* **1992**, *257*, 1661–1664.

[2] W. Cai, R. Morales-Martínez, X. Zhang, D. Najera, E. L. Romero, A. Metta-Magaña, A. Rodríguez-Fortea, S. Fortier, N. Chen, J. M. Poblet, L. Echegoyen, 'Single crystal structures and theoretical calculations of uranium endohedral metallofullerenes (U@C_{2n}, $2n = 74$, 82) show cage isomer dependent oxidation states for U', *Chem. Sci.* **2017**, *8*, 5282–5290.

[3] W. Cai, L. Abella, J. Zhuang, X. Zhang, L. Feng, Y. Wang, R. Morales-Martínez, R. Esper, M. Boero, A. Metta-Magaña, A. Rodríguez-Fortea, J. M. Poblet, L. Echegoyen, N. Chen, 'Synthesis and Characterization of non-Isolated-Pentagon-Rule Actinide Endohedral Metallofullerenes U@C_1(17418)-C_{76}, U@C_1(28324)-C_{80}, and Th@C_1(28324)-C_{80}: Low-Symmetry Cage Selection Directed by a Tetravalent Ion', *J. Am. Chem. Soc.* **2018**, *140*, 18039–18050.

[4] L. Bao, P. Peng, X. Lu, 'Bonding inside and outside Fullerene Cages', *Acc. Chem. Res.* **2018**, *51*, 810–815.

[5] P. W. Dunk, N. K. Kaiser, M. Mulet-Gas, A. Rodríguez-Fortea, J. M. Poblet, H. Shinohara, C. L. Hendrickson, A. G. Marshall, H. W. Kroto, 'The Smallest Stable Fullerene, M@C_{28} (M=Ti, Zr, U): Stabilization and Growth from Carbon Vapor', *J. Am. Chem. Soc.* **2012**, *134*, 9380–9389.

[6] R. F. Curl, R. C. Haddon, 'On the Formation of the Fullerenes', in 'The Fullerenes: New Horizons for the Chemistry, Physics and Astrophysics of Carbon', Eds. H. Kroto, D. Walton, Cambridge University Press, Cambridge, 1993, Vol. 343, pp. 19–32.

[7] P. W. Dunk, M. Mulet-Gas, Y. Nakanishi, N. K. Kaiser, A. Rodríguez-Fortea, H. Shinohara, J. M. Poblet, A. G. Marshall, H. W. Kroto, 'Bottom-up formation of endohedral monometallofullerenes is directed by charge transfer', *Nat. Commun.* **2014**, *5*, 5844.

[8] A. A. Popov, S. Yang, L. Dunsch, 'Endohedral Fullerenes', *Chem. Rev.* **2013**, *113*, 5989–6113.

[9] M. D. Diener, C. A. Smith, D. K. Veirs, 'Anaerobic Preparation and Solvent-Free Separation of Uranium Endohedral Metallofullerenes', *Chem. Mater.* **1997**, *9*, 1773–1777.

[10] R. D. Bolskar, J. M. Alford, 'Derivatization and solubilization of insoluble classes of fullerenes', US patent 0065206A1, 2003.

[11] M. Yamada, T. Akasaka, M. Nagase, 'Salvaging Reactive Fullerenes from Soot by Exohedral Derivatization', *Angew. Chem. Int. Ed.* **2018**, *57*, 13394–13405.

[12] C. Yeretzian, J. B. Wiley, K. Holczer, T. Su, S. Nguyen, R. B. Kaner, R. Whetten, 'Partial Separation of Fullerenes by Gradient Sublimation', *J. Phys. Chem.* **1993**, *97*, 10097–10101.

[13] M. D. Diener, J. M. Alford, 'Isolation of small-bandgap fullerenes and endohedral metallofullerenes', US patent 6303016B1, 2001.

[14] R. D. Bolskar, J. M. Alford, 'Purification of endohedral and other fullerenes by chemical methods', US patent 015716A1, 2003.

[15] S. Stevenson, G. Rice, T. Glass, K. Harich, F. Cromer, M. R. Jordan, J. Craft, E. Hadju, R. Bible, M. M. Olmstead, K. Maitra, A. J. Fisher, A. L. Balch, H. C. Dorn, 'Small-bandgap endohedral metallofullerenes in high yield and purity', *Nature* **1999**, *401*, 55–57.

[16] R. D. Bolskar, A. F. Benedetto, L. O. Husebo, R. E. Price, E. F. Jackson, S. Wallace, L. J. Wilson, J. M. Alford, 'First Soluble M@C_{60} Derivatives Provide Enhanced Access to Metallofullerenes and Permit in Vivo Evaluation of Gd@C_{60}[C$(COOH)_2]_{10}$ as a MRI Contrast Agent', *J. Am. Chem. Soc.* **2003**, *125*, 5471–5478.

[17] Y. Kubozono, H. Maeda, Y. Takabayashi, K. Hiraoka, T. Nakai, S. Kashino, S. Emura, S. Ukita, T. Sogabe, 'Extractions of Y@C_{60}, Ba@C_{60}, La@C_{60}, Ce@C_{60}, Pr@C_{60}, Nd@C_{60}, and Gd@C_{60} with Aniline', *J. Am. Chem. Soc.* **1996**, *118*, 6998–6999.

[18] T. Inoue, Y. Kubozono, S. Kashino, Y. Takabayashi, K. Fujitaka, M. Hida, M. Inoue, T. Kanbara, S. Emura, T. Uruga, 'Electronic structure of Eu@C_{60} studied by XANES and UV-VIS absorption spectra', *Chem. Phys. Lett.* **2000**, *316*, 381–386.

[19] T. Ogawa, T. Sugai, H. Shinohara, 'Isolation and Characterization of Er@C_{60}', *J. Am. Chem. Soc.* **2000**, *122*, 3538–3539.

[20] T. Kanbara, Y. Kubozono, Y. Takabayashi, S. Fujiki, S. Iida, Y. Haruyama, S. Kashino, S. Emura, T. Akasaka, 'Dy@C_{60}: Evidence for endohedral structure and electron transfer', *Phys. Rev. B* **2001**, *64*, 113403.

[21] Z. Wang, Y. Nakanishi, S. Noda, H. Niwa, J. Zhang, R. Kitaura, H. Shinohara, 'Missing Small-Bandgap Metallofullerenes: Their Isolation and Electronic Properties', *Angew. Chem. Int. Ed.* **2013**, *52*, 11770–11774.

[22] M. D. Diener, J. M. Alford, 'Isolation and properties of small-bandgap fullerenes', *Nature* **1998**, *393*, 668–671.

[23] A. Gromov, W. Krätschmer, N. Krawez, R. Tellgmann, E. B. Campbell, 'Extraction and HPLC purification of Li@$C_{60/70}$', *Chem. Commun.* **1997**, 2003–2004.

[24] X. Zhang, Y. Wang, R. Morales-Martínez, J. Zhong, C. de Graaf, A. Rodríguez-Fortea, J. M. Poblet, L. Echegoyen, L. Feng, N. Chen, 'U_2@I_h(7)-C_{80}: Crystallographic Characterization of a Long-Sought Dimetallic Actinide Endohedral Fullerene', *J. Am. Chem. Soc.* **2018**, *140*, 3907–3915.

[25] X. Zhang, W. Li, L. Feng, X. Chen, A. Hansen, S. Grimme, S. Fortier, D.-C. Sergentu, T. J. Duignan, J. Autschbach, S. Wang, Y. Wang, G. Velkos, A. A. Popov, N. Aghdassi, S. Duhm, X. Li, J. Li, L. Echegoyen, W. H. Schwarz, N. Chen, 'A diuranium carbide cluster stabilized inside a C_{80} fullerene cage', *Nat. Commun.* **2018**, *9*, 2753.

[26] K. Saïdane, M. Razafinimanana, H. Lange, A. Huczko, M. Baltas, A. Gleizes, J.-L. Meunier, 'Fullerene synthesis in the graphite electrode arc process: local plasma characteristics

and correlation with yield', *J. Phys. D Appl. Phys.* **2004**, *37*, 232–239.

[27] H. W. Kroto, 'The stability of the fullerenes C_n, with $n=24$, 28, 32, 36, 58, 60 and 70', *Nature* **1987**, *329*, 529–531.

[28] D. Sun, Z. Liu, X. Guo, W. Xu, S. Liu, 'High-Yield Extraction of Endohedral Rare-Earth Fullerenes', *J. Phys. Chem. B* **1997**, *101*, 3927–3930.

[29] Z. Slanina, S.-L. Lee, F. Uhlík, L. Adamowicz, S. Nagase, 'Computing relative stabilities of metallofullerenes by Gibbs energy treatments', *Theor. Chem. Acc.* **2007**, *117*, 315–322.

[30] Z. Slanina, S. Nagase, '$Sc_3N@C_{80}$: Computations on the Two-Isomer Equilibrium at High Temperatures', *ChemPhysChem* **2005**, *6*, 2060–2063.

[31] M. Mulet-Gas, L. Abella, M. R. Cerón, E. Castro, A. G. Marshall, A. Rodríguez-Fortea, L. Echegoyen, J. M. Poblet, P. W. Dunk, 'Transformation of doped graphite into cluster-encapsulated fullerene cages', *Nat. Commun.* **2017**, *6*, 1222.

[32] C.-H. Chen, L. Abella, M. R. Cerón, M. A. Guerrero-Ayala, A. Rodríguez-Fortea, M. M. Olmstead, X. B. Powers, A. L. Balch, J. M. Poblet, L. Echegoyen, 'Zigzag Sc_2C_2 Carbide Cluster inside a [88]Fullerene Cage with One Heptagon, $Sc_2C_2@C_s$ (hept)-C_{88}: A Kinetically Trapped Fullerene Formed by C_2 Insertion?', *J. Am. Chem. Soc.* **2016**, *138*, 13030–13037.

[33] G. te Velde, F. M. Bickelhaupt, E. J. Baerends, C. Fonseca Guerra, S. J. A. van Gisbergen, J. G. Snijders, T. Ziegler, 'Chemistry with ADF', *J. Comput. Chem.* **2001**, *22*, 931–967.

[34] S. Grimme, S. Ehrlich, L. Goerigk, 'Effect of the damping function in dispersion corrected density functional theory', *J. Comput Chem* **2011**, *32*, 1456–1465.

[35] M. Álvarez-Moreno, C. de Graaf, N. López, F. Maseras, J. M. Poblet, C. Bo, 'Managing the Computational Chemistry Big Data Problem: The ioChem-BD Platform', *J. Chem. Inf. Mode.* **2015**, *55*, 95–103.

Received February 7, 2019
Accepted March 20, 2019